Spatially correlated dynamics in a simulated glass-forming polymer melt: Analysis of clustering phenomena

Y. Gebremichael,[1,2,3] T. B. Schrøder,[1,*] F. W. Starr,[1] and S. C. Glotzer[1,3,†]

[1]*Center for Theoretical and Computational Materials Science and Polymers Division, National Institute of Standards and Technology, Gaithersburg, Maryland 20899*

[2]*Chemical Physics Program, Institute for Physical Sciences and Technology, University of Maryland, College Park, Maryland 20742*

[3]*Departments of Chemical Engineering and Materials Science and Engineering, University of Michigan, Ann Arbor, Michigan 48109*

(Received 5 March 2001; published 17 October 2001)

In recent years, experimental and computational studies have demonstrated that the dynamics of glass-forming liquids are spatially heterogeneous, exhibiting regions of temporarily enhanced or diminished mobility. Here we present a detailed analysis of dynamical heterogeneity in a simulated ''bead-spring'' model of a low-molecular-weight polymer melt. We investigate the transient nature and size distribution of clusters of ''mobile'' chain segments (monomers) as the polymer melt is cooled toward its glass transition. We also explore the dependence of this clustering on the way in which the mobile subset is defined. We show that the mean cluster size is time dependent with a peak at intermediate time, and that the mean cluster size at the peak time grows with decreasing temperature T. We show that for each T a particular fraction of particles maximizes the mean cluster size at some characteristic time, and this fraction depends on T. The growing size of the clusters demonstrates the growing range of correlated motion, previously reported for this same system [C. Beneman *et al.* Nature (London) **399**, 246 (1999)]. The distribution of cluster sizes approaches a power law near the mode-coupling temperature, similar to behavior reported for a simulated binary mixture and a dense colloidal suspension, but with a different exponent. We calculate the correlation length of the clusters, and show that it exhibits similar temperature- and time-dependent behavior as the mean cluster size, with a maximum at intermediate time. We show that the characteristic time of the maximum cluster size follows the scaling predicted by mode-coupling theory (MCT) for the β time scale, revealing a possible connection between spatially heterogeneous dynamics and MCT.

DOI: 10.1103/PhysRevE.64.051503 PACS number(s): 64.70.Pf

I. INTRODUCTION

The cooperative nature of molecular motion is considered one of the canonical features of liquids approaching their glass transition [1,2]. However, relatively few details are known concerning how and under what conditions cooperativity arises in these liquids, and in particular how cooperative motion is related to other canonical features of dense liquids and the glass transition. Numerous computational [3–18] and experimental [19–32] studies have demonstrated that dense liquids above their glass transition exhibit spatially heterogeneous dynamics (''dynamical heterogeneity''); that is, regions within the liquid exhibit enhanced or diminished mobility relative to the average on some time scale [32–36], which, depending on the system, type of experiment, and temperature T relative to the glass transition temperature T_g, can be less than, comparable to, or larger than the characteristic time for the decay of density fluctuations (the so-called α relaxation time τ_α). In some studies (e.g., NMR studies [19,20,27,28]), direct spatial information on the location of temporarily enhanced or reduced mobility molecules is lacking, but spatial correlation between dynamically similar molecules, and thus the existence of dynamically heterogeneous regions, can be inferred. In other studies (e.g., fluorescent probe studies [37,38]), more direct information about the existence and size of dynamically heterogeneous regions can be extracted.

In computer simulations [3–18] and microscopy studies of colloidal suspensions [30,31], where detailed information on the trajectories of individual model particles is directly accessible, the existence of dynamically heterogeneous regions has been directly observed and quantified. In these studies, the connection between dynamical heterogeneity and cooperativity, in which particles move together in the same direction in a correlated fashion, has been further elucidated [4,24,31,39]. For example, in Refs. [3–6], it was shown in a binary Lennard-Jones (LJ) mixture that at any given moment most particles can be found trapped in ''cages'' formed by their neighbors, while roughly 5–6 % constitute a highly mobile subset that is breaking out of these cages. It was further shown that these mobile, ''escaping'' particles move cooperatively in stringlike paths, forming clusters of strings which grow in size with decreasing temperature on approaching the mode-coupling temperature T_{MCT}, where T_{MCT} is the crossover temperature predicted by mode-coupling theory (MCT) [40] below which the dynamics are dominated by activated processes [41,42]. Typically, T_{MCT} is roughly $1.1T_g$–$1.5T_g$ [43]. The distribution of string lengths was found to be exponential, while the cluster size distribution $P(n)$ was found to follow a power law $P(n)\sim n^{-\tau}$ with $\tau\approx 2$. Recent experiments on suspensions of hard sphere colloids confirmed the clustering of a highly mobile subset of

*Present address: IMFUFA, Roskilde University, DK-4000 Roskilde, Denmark.

†Corresponding author. Electronic address: sglotzer@umich.edu

particles above the colloidal glass transition; $P(n)$ was found to obey a power law with roughly the same exponent [31]. They also confirmed the tendency for the cluster size to increase as the glass transition is approached.

In a recent study of the dynamics of a binary LJ mixture in terms of the potential energy surface [41], a preliminary attempt was made to connect cooperativity and dynamical heterogeneity to the potential energy landscape (PEL) description of glass-forming liquids [44]. In the PEL paradigm, the motion is partitioned into vibrations around stable potential energy minima and infrequent basin transitions that give rise to structural rearrangement. Reference [41] reported that, at sufficiently low T, transitions between basins of attraction on the potential energy surface are facilitated by particles moving in stringlike clusters, suggesting that cooperativity becomes a critical channel for relaxation at sufficiently low T.

In this paper we investigate the spatially heterogeneous motion of monomers in a bead-spring model of a cold, dense polymer melt. Our results are obtained by analyzing molecular dynamics simulations of a polymer melt [8,45]. Reference [8] showed via calculation of a ''displacement-displacement'' pair-correlation function that the dynamics of monomers is spatially correlated, that this correlation is time dependent, and that the amount of correlation increases rapidly as the melt is cooled. Here we take a different approach, similar to that taken in Refs. [5,6], and investigate the clustering of the most highly mobile monomers in any given time window. In this way we obtain additional insight into the spatially heterogeneous dynamics of the melt.

We show the transient nature and temperature dependence of the clusters formed by the mobile monomers, which is a result of the cooperative rearrangement of the monomers. We show that the mean cluster size, a measure of the extent of cooperativity, grows and shrinks during the time window when the mean square displacement of the monomers changes from the ballistic regime to the subdiffusive regime. Moreover, the maximum average cluster size grows with decreasing T. We show that the distribution of cluster sizes approaches a power law upon cooling toward the mode-coupling temperature. We also show that the correlation length of clusters exhibits a similar time and temperature behavior as the mean cluster size, demonstrating the existence of a growing length scale on cooling.

The paper is organized as follows. In Sec. II we briefly describe the model and simulation details. In Sec. III we investigate correlated motion by analyzing clusters of ''mobile'' monomers—i.e., those that undergo large displacements in a variable time interval Δt. We calculate the size of the clusters and compare different methods of choosing mobile monomers. In Secs. IV and V we analyze the behavior and distribution of clusters as a function of time and temperature. In Sec. VI we calculate a correlation length for the clusters, and demonstrate its time-dependent nature. A discussion and summary follow in Secs. VII and VIII.

II. MODEL AND SIMULATION

We study a system of 120 polymer chains modeled by a coarse-grained, bead-spring description. Each chain is composed of ten monomers (beads) with mass m set to unity. Monomers are modeled as Lennard-Jones particles (with potential $V_{\mathrm{LJ}}=4\epsilon[(\sigma/r)^{12}-(\sigma/r)^{6}]$) with a finitely extensible, nonlinear elastic (FENE) potential ($V_{\mathrm{FENE}}=-(k/2)R_0^2\ln[1-(r/R_0)^2]$) connecting nearest neighbors along a chain [48,49]. The parameters ϵ and σ in the LJ potentials are set to unity. The parameters of the FENE potential are chosen as $k=30$ and $R_0=1.5$, producing relatively stiff bonds, and preventing crystallization at lower temperatures due to the presence of incompatible preferred length scales (which correspond to the positions of the minima of the pure LJ potential for nonbonded monomers and the combined LJ + FENE potential for bonded monomers). We analyze the simulations of Refs. [8,45], consisting of eight state points with average pressure $p=1$, and temperature T ranging from 0.46 to 0.7. (Here, and in the remainder of the paper, all units are quoted in reduced units; length in units of σ, temperature T in units of ϵ/k_B, time in units of $\sigma\sqrt{m/\epsilon}$). The density ρ is adjusted between $0.98\leqslant\rho\leqslant1.04$ in order to follow an isobaric path. All quantities presented here are calculated by averaging between 150 and 200 independent configurations, except for the lowest temperature where we used 60 independent configurations for averaging.

As described in Refs. [8,45], the system is equilibrated at all thermodynamic state points by allowing each chain to propagate several times the distance of the radius of gyration before any trajectories were stored. Additionally, we carefully checked that the time correlation functions calculated from these trajectories are independent of the time origin chosen, and decay to zero within the time scale of the simulations. In this way, we confirm that there is no aging or other nonequilibrium behavior that might skew our results. References [8,45] found that the mode-coupling temperature for this system is $T_{\mathrm{MCT}}=0.45\pm0.01$, and $T_0=0.34\pm0.02$ [45], the so-called ideal glass transition temperature estimated from the Vogel-Tammann-Fulcher (VTF) equation, which is typically close to the Kauzmann temperature T_{K}, the temperature where the extrapolated liquid and crystal entropy are equal [1,43]. More details of the simulation may be found in Refs. [8,45].

III. CALCULATION OF MEAN CLUSTER SIZE

In the cooled liquid we study, it is known from, e.g., calculations of the mean square displacement $\langle r^2(\Delta t)\rangle$, that at intermediate times monomers on average are trapped or localized in cages formed by their neighbors (Fig. 1). In a similar model glass-forming binary LJ mixture, it was demonstrated that at any given time most of the particles can be found oscillating in these cages, with only approximately 5–6 % of the particles undergoing significant displacement at that time. At a later time, of course, a different subset of particles can be found moving beyond their cage. In the range of T studied in that work, however, as in the present study, the distribution of particle (or monomer) displacements as measured by the self van Hove distribution function is continuous and unimodal, exhibiting at most a long tail to large displacements (in some liquids, this tail becomes a secondary peak at sufficiently low T [46]). This makes the iden-

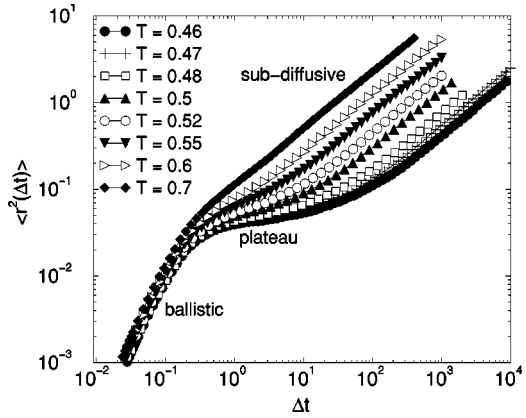

FIG. 1. Monomer mean square displacement $\langle r^2(\Delta t)\rangle$ for several temperatures showing ballistic, plateau, and subdiffusive regimes. The subdiffusive regime is followed at late time by a diffusive regime (not shown).

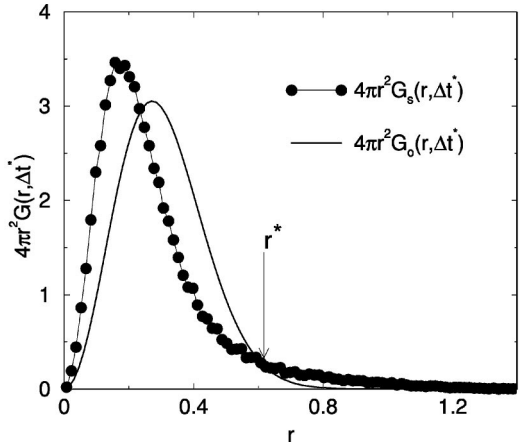

FIG. 2. The radially averaged van Hove correlation function $G_s(r,\Delta t)$ at $\Delta t=\Delta t^*$ for $T=0.46$, plotted with the Gaussian distribution $G_0(r,\Delta t^*)$. Mobile monomers are defined as those monomers that, during Δt, moved a distance greater than r^*.

tification of mobile particles substantially more difficult than if the distribution of particle displacements were, say, bimodal, in which case there would be a clearly motivated criterion for identifying mobile particles.

Our goal in this section is to determine an appropriate method of choosing the most mobile monomers in a time interval Δt in order to best establish the nature of dynamical heterogeneity in our model liquid. To do this, we will ask whether there is a subset of mobile monomers that forms clusters as in the LJ liquid studied in Refs. [3,5,6] and the colloidal liquids studied in Refs. [30,31], and, if so, how should this subset be chosen? To answer these questions, we will compare two methods of identifying the appropriate subset of monomers. We first apply a method that utilizes the crossing point of the self van Hove distribution function and Gaussian distribution function as a reference displacement for identifying the most mobile monomers in a given interval of time, as used in Refs. [3–6]. In the second method, we again consider the most mobile monomers in a given time interval, but we vary the fraction of monomers included in the subset, choosing the fraction that shows the strongest tendency for clustering. For both methods, we investigate the time and temperature dependence of clusters formed by these monomers, focusing on the time window where $\langle r^2(\Delta t)\rangle$ exhibits ballistic, plateau, and subdiffusive regimes (Fig. 1) [47]. We also investigate the distribution of cluster sizes of mobile monomers, and the time and temperature dependence of this distribution.

A. Fixed fraction

Previous studies [3,5,6] identified the mobile subset as those particles that, in an interval Δt^*, move further than some distance r^*. Specifically, Δt^* is defined as the time interval when the non-Gaussian parameter $\alpha_2(\Delta t)$, which measures the degree to which the distribution of particle displacements differs from Gaussian, is maximum [50]. The quantity r^* is defined as the crossing point of the self part of the van Hove correlation function [51]

$$G_s(\mathbf{r},\Delta t)=\frac{1}{N}\left\langle \sum_{i=1}^{N} \delta(\mathbf{r}_i(\Delta t)-\mathbf{r}_i(0)-\mathbf{r})\right\rangle, \qquad (1)$$

which measures the probability density of particle displacements, and the Gaussian distribution

$$G_0(r,\Delta t)=\left(\frac{3}{2\pi\langle r^2(\Delta t)\rangle}\right)^{3/2}\exp\left(\frac{-3r^2}{2\langle r^2(\Delta t)\rangle}\right), \qquad (2)$$

calculated with the measured value of $\langle r^2(\Delta t)\rangle$ at $\Delta t=\Delta t^*$.

In Fig. 2, we plot $G_s(r,\Delta t^*)$ and $G_0(r,\Delta t^*)$ to identify r^*. The fraction ϕ of the monomers that are mobile is defined by integrating $G_s(r,\Delta t^*)$ for $r\geq r^*$, i.e.,

$$\phi\equiv\int_{r^*}^{\infty}4\pi r^2 G_s(r,\Delta t^*)dr. \qquad (3)$$

Using this method on a binary LJ mixture, ϕ was found to constitute approximately 5.5% of the total number of particles, independent of T and ρ [3–6]. Following the same procedure, we find $6.2\%\leqslant\phi\leqslant 6.8\%$ (Table I). Thus for convenience we will use an intermediate value of $\phi=6.5\%$ for studies with a fixed fraction of mobile monomers.

Once ϕ is selected, the subset of monomers that is considered mobile in each time interval Δt is identified by ranking the scalar displacement of all monomers in Δt, and choosing the 6.5% with the largest value. In any given Δt, the number of mobile monomers defined in this way is necessarily the same, but the membership will generally be different since a monomer that is mobile in one time interval may be caged in the next, and vice versa.

We define clusters [5,6] as groups of highly mobile monomers that are within the first neighbor shell of each other [52], where the first neighbor shell is defined by the distance of the first minimum ($r=1.5$) of the pair correlation function $g(r)$ [51,53]. An example of the clusters formed by the 6.5% most mobile monomers is shown for $T=0.46$ at early Δt

TABLE I. ϕ^I refers to the fraction ϕ of highly mobile monomers at a time Δt^* when α_2 is maximum (Sec. III A), and ϕ^{II} refers to the fraction that maximizes the normalized weight-averaged cluster size for each T (Sec. III B). At each T, $\phi < \phi_c$, where ϕ_c is the value of ϕ at the percolation threshold (see Appendix A). The normalization factor S_0 is the initial (or, correspondingly, the random) value of the weight-averaged cluster size of the fraction considered. S_0^I refers to the value of S_0 at each T for $\phi = 6.5\%$, used to evaluate $S(\Delta t)$ using the procedure outlined in Sec. III A. S_0^{II} refers to the value of S_0 at each T for a fraction corresponding to ϕ^{II}. Note that S_0^I is nearly constant, $S_0^I = 2.65 \pm 0.1$ for all T, while S_0^{II} varies considerably because ϕ is different for each state point. The error bars in calculating ϕ^I reflect the uncertainty in estimating r^* for the evaluation of ϕ from Eq. (3). The error bars in estimating ϕ^{II} reflect the range of ϕ over which the fraction that maximizes S could be identified with confidence.

T	0.46	0.47	0.48	0.5	0.52	0.55	0.6	0.7
ϕ^I	$6.4 \pm 0.5\%$	$6.2 \pm 0.4\%$	$6.8 \pm 0.5\%$	$6.5 \pm 0.3\%$	$6.7 \pm 0.6\%$	$6.7 \pm 0.6\%$	$6.5 \pm 0.7\%$	$6.3 \pm 0.7\%$
ϕ^{II}	$5 \pm 1\%$	5.5 ± 0.5	$5.5 \pm 0.5\%$	$6 \pm 1\%$	$6.5 \pm 0.5\%$	$7 \pm 1\%$	$7.5 \pm 0.5\%$	$8 \pm 1\%$
S_0^I	2.66 ± 0.05	2.58 ± 0.02	2.7 ± 0.03	2.55 ± 0.02	2.64 ± 0.01	2.61 ± 0.01	2.76 ± 0.03	2.62 ± 0.02
S_0^{II}	2.06 ± 0.06	2.22 ± 0.16	2.26 ± 0.2	2.36 ± 0.04	2.64 ± 0.24	2.81 ± 0.53	3.27 ± 0.26	3.31 ± 0.03
ϕ_c	$7.1 \pm 0.4\%$	$8 \pm 0.2\%$	$7.4 \pm 0.1\%$	$8.2 \pm 0.1\%$	$8.8 \pm 0.2\%$	$9 \pm 0.3\%$	$9.8 \pm 0.1\%$	$10.6 \pm 0.1\%$

[Fig. 3(a)], and at intermediate Δt [Fig. 3(b)]. We see that the typical cluster size depends upon the time window of observation Δt; smaller clusters appear at early Δt, and larger clusters appear at intermediate Δt, when $\langle r^2(\Delta t)\rangle$ crosses over from the plateau regime to the subdiffusive regime. Such transient clustering of mobile particles has also been observed experimentally in dense colloidal suspensions using a confocal microscope [31], by looking at the (roughly) 5% most mobile particles as in Refs. [5,6].

To quantify the clustering of mobile monomers, we calculate the weight-averaged mean cluster size [54],

$$S_w(\Delta t) = \frac{\langle n^2(\Delta t)\rangle}{\langle n(\Delta t)\rangle} = \frac{\sum n^2(\Delta t) P(n(\Delta t))}{\sum n(\Delta t) P(n(\Delta t))}. \qquad (4)$$

Here $P(n)$ is the probability of finding a cluster of size n, and $nP(n)$ is the probability that a randomly chosen mobile monomer belongs to a cluster of size n. $S_w(\Delta t)$ defined in this way is the average size of a cluster to which a randomly chosen mobile monomer belongs.

We normalize S_w by the average size S_0 of clusters formed by mobile monomers at the initial Δt (i.e., one molecular dynamics time step), and find that, at each T, S_0 (reported in Table I) coincides with the average cluster size found by selecting monomers randomly [55]. This demonstrates that short-time monomer motion is uncorrelated, as found previously for this system using an alternative (non-cluster-based) analysis approach [8], and as found in both the LJ liquid referred to previously [7] and a colloidal suspension [30,31]. Following convention [5,54], any spanning clusters present in a given snapshot are omitted from the calculation to minimize finite size effects. In Fig. 4, we show the normalized mean cluster size $S \equiv S_w/S_0$ for several T. We find that the clusters formed by the most mobile monomers ''grow'' and ''shrink'' as the window of observation increases. Furthermore, the maximum amplitude of $S(\Delta t)$ shown in the inset of Fig. 4 increases with decreasing T,

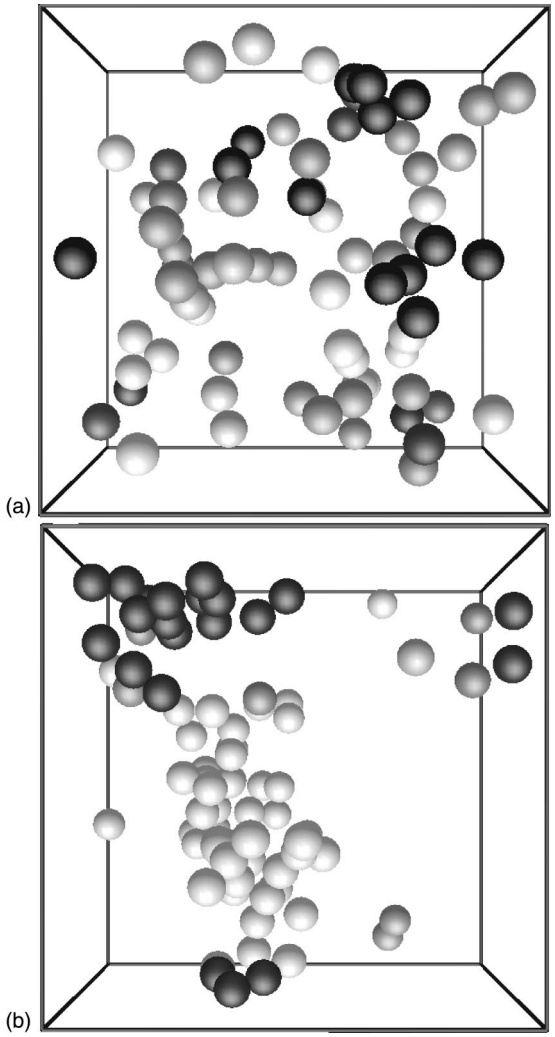

FIG. 3. Clusters formed by the 6.5% most mobile monomers (a) at early time ($\Delta t = 0.002$) and (b) at intermediate time ($\Delta t = 45.4$), for $T = 0.46$. Each monomer is represented as a sphere, and connectivity information has been suppressed. Monomers belonging to the same cluster are colored the same shade of gray. Note that only the most mobile monomers out of the 1200 total monomers are shown in the figure.

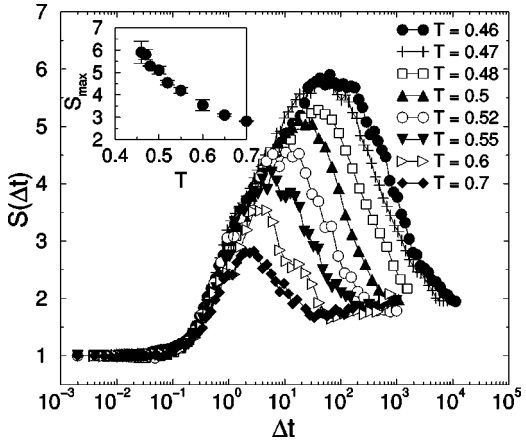

FIG. 4. Normalized mean cluster size $S(\Delta t)$ for $\phi = 6.5\%$ for all T. The inset shows $S_{\max} \equiv S(\Delta t_{\max})$ versus T, where $\Delta t_{\max}$ is the time at which S is maximal. Actual (unnormalized) cluster sizes are nearly three times larger than those shown.

indicating that the monomer motion becomes increasingly spatially correlated as the melt becomes colder and more dense.

The behavior of $S(\Delta t)$ can be interpreted by comparing with $\langle r^2(\Delta t)\rangle$ (Fig. 1). Consider, for example, the behavior of S at $T=0.46$. For small Δt ($\Delta t \lesssim 2\times 10^{-1}$), the monomers' motion is ballistic, and so the probability of finding large clusters is negligibly small, since we are simply choosing the most highly mobile monomers from the tail of the Maxwell-Boltzmann velocity distribution, and these monomers are randomly distributed in space; at these short times $G_s(r,t)$ is well approximated by a Gaussian. At slightly longer Δt ($2\times 10^{-1} \lesssim \Delta t \lesssim 10$, the plateau regime) the motion of monomers is restricted to ''rattling'' within the cage formed by neighboring monomers. Thus, big clusters are less likely to be formed since the particles do not move large distances, and are consequently less likely to affect the motion of others. Between the plateau and subdiffusive regimes ($10 \lesssim \Delta t \lesssim 10^3$), when the monomers begin to escape from their cages [11], the motion of one monomer becomes highly influenced by the motion of others around it; a monomer cannot move unless its neighbors also move, causing large clusters to be formed.

At the longest time scale we probe ($\Delta t \gtrsim 10^3$), the monomers' displacement is subdiffusive (characterized by $\langle r^2(t)\rangle \sim t^{0.62\pm 0.03}$) [45,56]. At this time scale, the probability of finding large clusters again decreases, indicating an increased tendency toward uncorrelated motion. Nevertheless, $S_w(\Delta t)$ is still greater than the random value S_0. This may be due to the presence of some persistent correlation since the monomers are not yet completely diffusive, or possibly to polymer specific effects, or both; we postpone further discussion of this long-time behavior to future investigation. We note that during this time scale, while the motion of monomers becomes uncorrelated and their displacement is subdiffusive, the fraction of mobile monomers comprised of end monomers significantly increases from its mean field value $f_{\text{end}} \approx 0.2$ in the ballistic or the plateau regime (see Appendix B for detailed discussion of the contribution of end monomers to the mobile subset).

The behavior of $S(\Delta t)$ is qualitatively similar to that of a generalized susceptibility $\kappa_U(\Delta t)$ calculated for this same system in Ref. [8]. κ_U is related to the volume integral of the displacement-displacement correlation function (essentially a density-density correlation function, but with every particle's contribution weighted by its scalar displacement in Δt) in the same way as the isothermal compressibility κ_T in a fluid is related to the volume integral of the density-density correlation function. Accordingly, $\kappa_U(\Delta t)$ is proportional to the fluctuations in the total system displacement at time Δt, in the same way as κ_T is proportional to the fluctuations in the number of particles in the fluid.

The similarity between S and κ_U is not surprising, since the scalar displacements of the most highly mobile monomers in Δt are included in κ_U. However, the peak time of $S(\Delta t)$, which coincides with the crossover between the plateau and subdiffusive regimes, precedes that of $\kappa_U(\Delta t)$ (by less than a factor of 10 at $T=0.46$). This suggests that the cooperative motion of monomers, which requires clustering and allows the monomers to escape from their cages, is a precursor to the more global dynamical heterogeneity measured by κ_U.

B. Variable fraction

The method outlined in the last section for selecting a fraction of mobile monomers ensures a clearly defined and reproducible subset of the most mobile monomers in a given time window, and can be easily applied to any system. However, there is no *a priori* reason why this should be the definition of choice, and in particular whether this fraction is more spatially correlated than some other fraction. The ''ideal'' fraction is the one that most clearly and naturally captures dynamical correlation. To search for this ''natural'' fraction, and to check if it is substantially different from the fraction used in the previous section, we select a subset of highly mobile monomers by varying ϕ, and then choosing that fraction that maximizes $S(\Delta t)$ for all Δt.

We find that $S(\Delta t)$ is maximum for ϕ in the range 5%–8% for all T considered, e.g., S is maximum at $\phi = 5\%$ for $T=0.46$ and at 8% for $T=0.7$. Table I shows a complete list of fractions ϕ^{II} that maximize S at each T. In Fig. 5 we show $S(\Delta t)$ for $T=0.46$ and $T=0.7$ for four values of ϕ. We have checked S at 1% intervals of ϕ to determine the fraction ϕ that maximizes $S(\Delta t)$. However, for the sake of clarity, we show only a few representative ϕ, including the ϕ that yields a maximal value of S.

Using those fractions ϕ^{II} reported in Table I that maximize the cluster size for each T, we calculate $S(\Delta t)$ for each T, as shown in Fig. 6. We find that this second method does not alter the qualitative features of the time and temperature dependence of S found by the first method. However, there are slight quantitative differences in the values of S. The peak values of S obtained from the variable fraction method are slightly larger (at most by $\approx 13\%$) than the method that at each T uses fixed $\phi = 6.5\%$. Since this difference in S from the two methods is not dramatic, we perform all subsequent analysis using a fixed fraction $\phi = 6.5\%$ for all T.

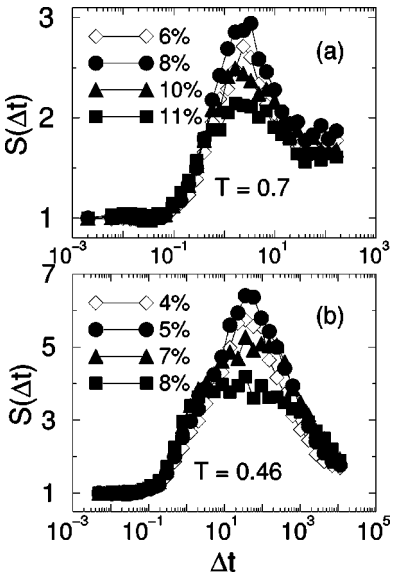

FIG. 5. Normalized weight-averaged cluster size $S(\Delta t)$ as a function of time window for selected ϕ for (a) $T=0.7$, and (b) $T=0.46$. For these two state points, $S(\Delta t)$ is maximized by $\phi=8\%$ and $\phi=5\%$, respectively. Only a few selected fractions are shown for the clarity of the graph.

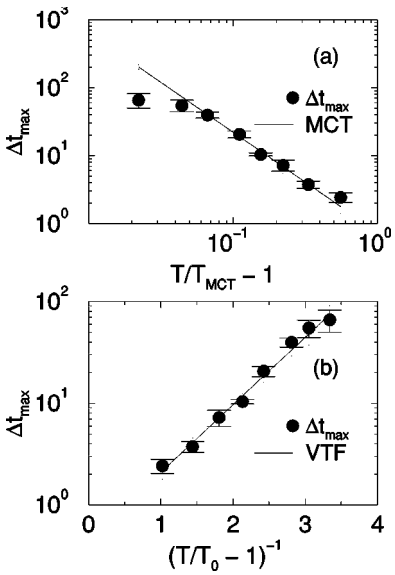

FIG. 7. Temperature dependence of $\Delta t_{\max}$, using the top 6.5% mobile monomers, fitted to (a) a power law [Eq. (5)], with $T_{\mathrm{MCT}}=0.45$, yielding $\gamma=1.47\pm0.16$, and (b) a VTF expression [Eq. (6)], yielding $E=0.54\pm0.07$ and $T_0=0.35\pm0.02$ plotted on linear-logarithmic axes.

IV. TEMPERATURE DEPENDENCE OF PEAK AVERAGE CLUSTER SIZE

We next focus on the temperature dependence of the maximum value $S_{\max}$ of $S(\Delta t)$, and the time $\Delta t_{\max}$ at which $S(\Delta t)$ is maximum. Examination of Fig. 1 shows that $\Delta t_{\max}$ is in the time window when monomers escape from their cages, as indicated by the increase of $\langle r^2(\Delta t)\rangle$ from the plateau toward the subdiffusive regime; this time also corresponds roughly to the β relaxation regime [40]. The shift in $\Delta t_{\max}$ to longer Δt as T decreases reflects the increase in the time scale necessary for a monomer to break free from its cage, which requires the participation of larger groups of monomers on increased cooling toward T_g. At each T, this peak time is close to, but slightly earlier than, the time scale where $\alpha_2(\Delta t)$ is maximum.

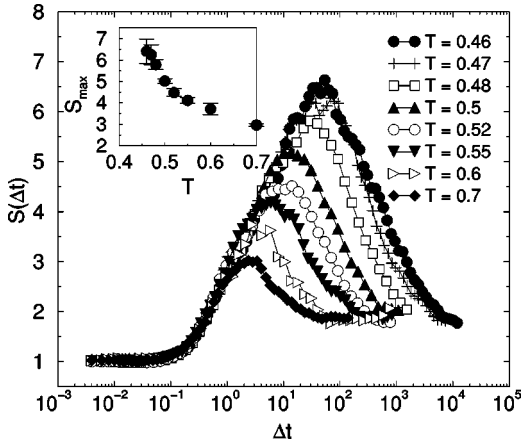

FIG. 6. Normalized weight-averaged cluster size as a function of time for different temperatures using the fraction ϕ of mobile monomers that provides the largest average cluster for the given temperature. The inset shows $S_{\max}\equiv S(\Delta t_{\max})$ versus T, where $\Delta t_{\max}$ is the time at which S is maximal. Actual (unnormalized) cluster sizes are nearly three times larger than those shown.

The T dependence of $\Delta t_{\max}$ can be studied by fitting the data by various functional forms. One choice is to fit the data by a power law. In the temperature regime we study, other characteristic times, such as τ_α, follow power law behavior, as predicted by the mode-coupling theory [40]. Additionally, the time t^* when the non-Gaussian parameter is maximum has been found to follow a power law in $(T-T_{\mathrm{MCT}})$ [57]. Also, Ref. [8] found that the time when the correlations as measured by a displacement-displacement correlation function are maximum, can be fitted by a power law in $(T-T_{\mathrm{MCT}})$. Motivated by these findings, we fitted the data by

$$\Delta t_{\max}\sim(T-T_{\mathrm{MCT}})^{-x}. \tag{5}$$

Figure 7(a) shows the best fit obtained by fixing $T_{\mathrm{MCT}}=0.45$. $\Delta t_{\max}$ shows a reasonable power law behavior with $x=1.47\pm0.16$ in the temperature regime where MCT holds. The deviation from power law at the lowest T, which is commonly observed for dynamical quantities, is expected due to the breakdown of MCT near T_{MCT} [58,59].

MCT predicts the β time scale t_ϵ satisfies the relation $t_\epsilon\sim(T-T_{\mathrm{MCT}})^{-1/2a}$ where a is uniquely determined by fixing any other exponent used by MCT. However, unambiguous identification of a time scale that has the predicted scaling of t_ϵ has been notoriously difficult in simulations of supercooled liquids [60]. Within a MCT analysis of the same simulation data examined here, Ref. [45] found that $\gamma=1.95$, and so MCT predicts $a=0.352$, and thus $1/2a=1.42$, which is within numerical uncertainty of the exponent x determined from $\Delta t_{\max}$. Thus, $\Delta t_{\max}$ follows the predicted scaling law for the β time scale, and exposes an un-

TABLE II. Fitting parameters for $\Delta t_{\max}$ and τ_α obtained from the power law and VTF fits. The exponents are results from a fit using the power law of Eq. (5) with $T_{\rm MCT}=0.45$ fixed, as estimated from previous work [8,45]. The parameters T_0 and E are results of fitting using the VTF form in Eq. (6). Our results for T_0 are consistent with the value $T_0=0.34\pm0.02$ reported in [45].

	Exponent	T_0	E
$\Delta t_{\max}$	1.47 ± 0.16	0.35 ± 0.02	0.54 ± 0.07
τ_α	1.95 ± 0.15	0.34 ± 0.02	0.93 ± 0.1

expected, although perhaps not surprising, connection between dynamical heterogeneity and MCT. The correspondence of $\Delta t_{\max}$ with t_ϵ, and the fact that $\Delta t_{\max}$ and τ_α would appear to diverge at the same temperature if the functional forms continued to hold to lower T, suggests that the two time scales represent a hierarchy of events in the relaxation process, consistent with the MCT prediction of two time scale relaxation process.

Another functional form for the T dependence of dynamical quantities that often holds in supercooled liquids is given by the well known Vogel-Tammann-Fulcher equation [1]

$$\Delta t_{\max}\sim\exp\left(\frac{E}{T-T_0}\right). \tag{6}$$

The fit of this expression to the data is shown in Fig. 7(b). We find a reasonable agreement with the VTF form with $T_0=0.35\pm0.02$; this value agrees with the value $T_0=0.34\pm0.02$ found by fitting τ_α, defined as the time at which the incoherent (self) part of the intermediate scattering function $F_q^{inc}(\tau_\alpha)=0.3$ [45]. Note that τ_α occurs at a later time than $\Delta t_{\max}$. The numerical results for these quantities are summarized in Table II.

The observation of a growing cluster size shown in the insets of Figs. 4 and 6 is consistent with the results of Ref. [5], and with earlier hypotheses that dynamics in supercooled fluids involves the motion of molecules within ''cooperatively rearranging regions'' [61–66], whose size grows as the glass transition is approached on cooling. In the Adam-Gibbs theory [61], the smallest possible size z^* that can give rise to a cooperative rearrangement is inversely proportional to the configurational entropy of the system [1], which is a measure of the number of mechanically stable states sampled by the system. The direct connection between z^* and the mean cluster size of mobile monomers in our analysis is not immediately evident. However, we can discuss the implications of growing cluster sizes in the spirit of the Adam-Gibbs theory, which has proved to be useful for the interpretation of transport and relaxation in supercooled liquids [67–71].

The Adam-Gibbs theory predicts that a thermodynamic glass transition occurs at a finite T as the configurational entropy vanishes. As a consequence, the theory also predicts that z^* diverges at nonzero temperature. However, our result for $S_{\max}\equiv S(\Delta t_{\max})$ showing Arrhenius T (i.e., VTF with $T_0=0$, Fig. 8) dependence over the (admittedly narrow) range of temperatures we have simulated implies that the mean

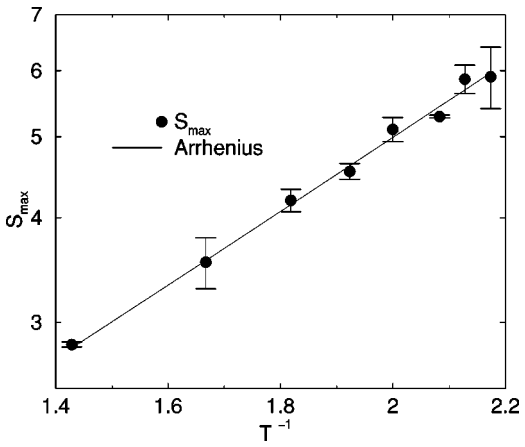

FIG. 8. Temperature dependence of $S_{\max}$ fitted to the Arrhenius form $S_{\max}\sim\exp(E/T)$, with $E=0.98\pm0.02$, plotted on semilogarithmic axes (logarithm of $S_{\max}$).

cluster size does not diverge at nonzero temperature [72]. This may indicate that the T range studied is too far from T_g to reliably estimate the T at which S might diverge. Alternatively, $S_{\max}$ may not be an appropriate measure of z^*, since $S_{\max}$ measures the *average* size of clusters formed by the mobile monomers that move in a cooperative manner (the ''max'' refers to the fact that there is a time scale on which S is maximal), while z^* is the *minimum* size of cooperatively rearranging regions of the entire system. Additionally, we find that S depends on the time window of observation while the time dependence of z^* is not defined.

V. CLUSTER SIZE DISTRIBUTION $P(n)$

In the previous section, we examined the average cluster size S. Here we examine the cluster size distribution $P(n)$, and study both the time and temperature dependence of this quantity. We first consider $P(n)$ at the lowest temperature ($T=0.46$) for several Δt [Figs. 9(a) and 9(b)]. At early

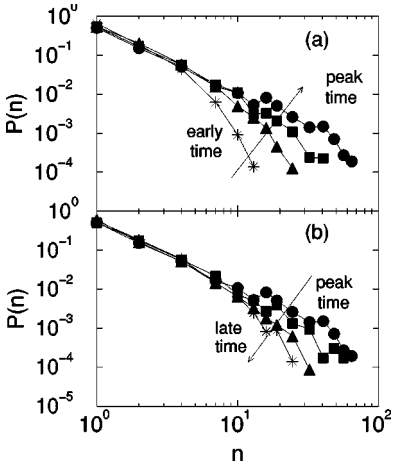

FIG. 9. Probability distribution $P(n)$ of cluster sizes at $T=0.46$ for different times as time progresses (a) from early time ($\Delta t=0.02$) to the peak time ($\Delta t=65.9$), and (b) from the peak time ($t=65.9$) to the subdiffusive regime ($\Delta t=11\,939.5$).

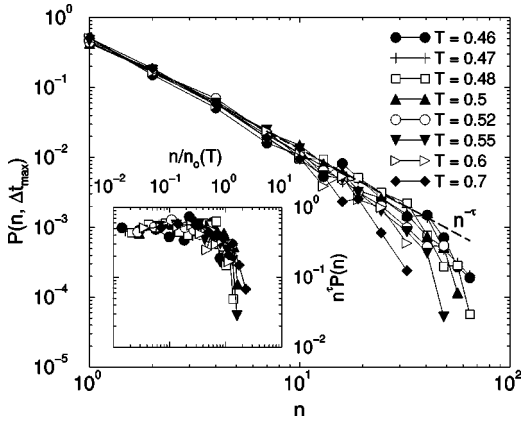

FIG. 10. $P(n,\Delta t_{\max})$ for the 6.5% most mobile monomers as a function of cluster size n for different T. The dashed line is a simple power law fit $P(n)\sim n^{\tau}$ with $\tau=1.62$ for $T=0.46$. The inset shows the same data scaled as indicated to show data collapse.

times, we find that $P(n)$ is dominated by smaller clusters, as expected from the fact that $S(\Delta t)$ is small at early Δt. As Δt increases through the plateau regime of $\langle r^2(\Delta t)\rangle$ (Fig. 1), larger clusters contribute significantly to $P(n)$. As Δt continues to increase into the subdiffusive regime, $P(n)$ again becomes dominated by small clusters.

We now compare $P(n)$ for different T at the characteristic time $\Delta t_{\max}$. Figure 10 shows that as T decreases $P(n,\Delta t_{\max})$ becomes dominated by larger clusters. This is a consequence of correlated motion of monomers as T approaches T_{MCT}, which is expected from the behavior of $S(\Delta t)$ presented earlier. We find that $P(n,\Delta t_{\max})$ can be fitted by a power law with exponential cutoff [54],

$$P(n)\sim n^{-\tau}\exp[-n/n_0(T)] \tag{7}$$

where $n_0(T)$ is a characteristic cluster size for the given T. The corresponding data collapse is shown in the inset of Fig. 10. The collapse is not nearly as good as for the larger system studied in Ref. [5], which may be due to finite size effects. Figure 11 shows that $n_0(T)$ increases as T decreases, causing the probability distribution to approach a simple power law with decreasing T. We find $\tau=1.62\pm0.12$ for all T. This value is smaller than the value obtained for a binary mixture of LJ particles ($\tau\approx1.9$) [5], and for colloids ($\tau=2.2\pm0.2$) [31], suggesting that the exponent value may be nonuniversal.

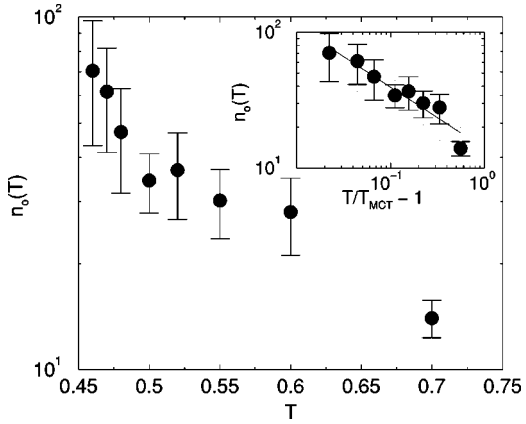

FIG. 11. A cutoff cluster size $n_0(T)$ obtained from fitting Eq. (7) to the data, plotted as a function of T. The error bar is estimated by fixing $\tau=1.62$, and then determining the range of n_0 values in Eq. (7) that reasonably fit the $P(n)$ data. Inset: a power law fit to $n_0(T)$ data, i.e., $n_0(T)\sim(T-T_{\mathrm{MCT}})^{-\gamma}$, using $T_{\mathrm{MCT}}=0.45$. The value of γ obtained from the fit is $\gamma=0.45\pm0.08$.

VI. DYNAMIC CORRELATION LENGTH

It is straightforward to calculate the correlation (or connectivity) length ξ of the clusters analyzed in the previous section. In lattice percolation theory, the correlation or connectivity length ξ, given by

$$\xi^2=\frac{\sum r^2 g(r)}{\sum g(r)}, \tag{8}$$

is defined as the root-mean-square distance between two sites belonging to the same cluster [54], where r is the distance between two sites and $g(r)$ is the pair correlation or pair connectivity function, defined as the probability that a site a distance r from an occupied site belongs to the same cluster. To map this definition onto the off-lattice system we consider, we define ξ as the root-mean-square distance between two monomers in a cluster, where $g(r)$ is the probability that a monomer a distance r from another monomer belongs to the same cluster. The sum in Eq. (8) runs over all monomers in the cluster.

Equation (8) may be rewritten in terms of the cluster size n and the radius of gyration R_n as [54]

$$\xi^2=\frac{2\sum R_n^2 n^2 P(n)}{\sum n^2 P(n)}. \tag{9}$$

R_n is defined by

$$R_n=\frac{\sum_i \sum_j |\mathbf{r}_i-\mathbf{r}_j|^2}{2n^2}, \tag{10}$$

where $\mathbf{r}_i$ and $\mathbf{r}_j$ refer to the positions of monomers i and j, where i and j are within the same cluster.

Figure 12(a) shows the dynamic correlation length $\xi(\Delta t)$ for several T. We find that $\xi(\Delta t)$ exhibits a time and temperature dependence similar to that of $S(\Delta t)$ [Fig. 12(b)], i.e., it grows and shrinks with Δt, and indicates a dynamic correlation length that increases on cooling. This similarity is not surprising since ξ is related to the average radius of the clusters that contribute significantly to S [54]. At the largest Δt accessible to our simulations, $\xi(\Delta t)$ does not decay to the initial value, also observed for S. The maximum value of $\xi(\Delta t)$ appears to saturate to the same value of approximately

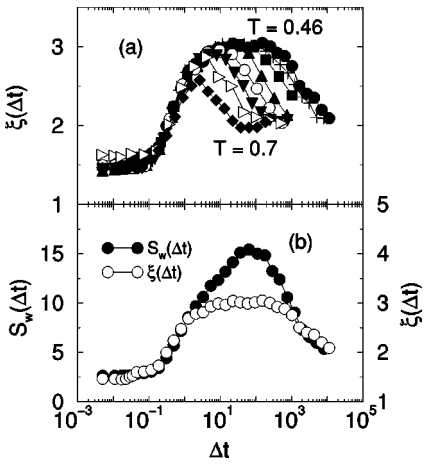

FIG. 12. (a) Dynamic correlation length $\xi(\Delta t)$ for different T. (b) $S_w(\Delta t)$ plotted together with $\xi(\Delta t)$ for $T=0.46$ to emphasize that both quantities increase and decrease on the same time scale. Note that here the mean cluster size is not normalized by S_0.

$\xi_{max} \approx 3.1$ for $T \lesssim 0.5$. This saturation is likely due to the small system size of the simulation, since the maximum value of ξ for these temperatures approaches half the system length ($L/2 \approx 5.25$) in our simulation. Indeed, finite size effects have been reported for simulation studies of dynamical heterogeneity, and in many of the configurations examined in the present work clusters were found that spanned the entirety of the simulation box. In Fig. 13 we plot $\xi(\Delta t_{max})$ as a function of T. The correlation length may also be limited by the radius of gyration of the chains. It is clear from Fig. 13 that we do not detect a tendency toward divergence of ξ in the temperature range studied. Larger systems and lower T, which are outside the scope of the present study, are needed to explore additional growth of ξ.

VII. DISCUSSION

In Sec. V, we fitted the cluster size distribution function $P(n)$ by a power law with an exponential cutoff, and we found a value of $\tau < 2$, whereas classical percolation theory implies $\tau > 2$ [54]. This discrepancy could be due to the finite

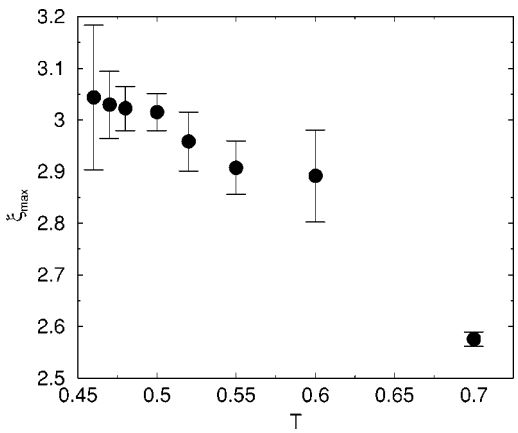

FIG. 13. Dynamic correlation length $\xi(\Delta t_{max})$ as a function of T.

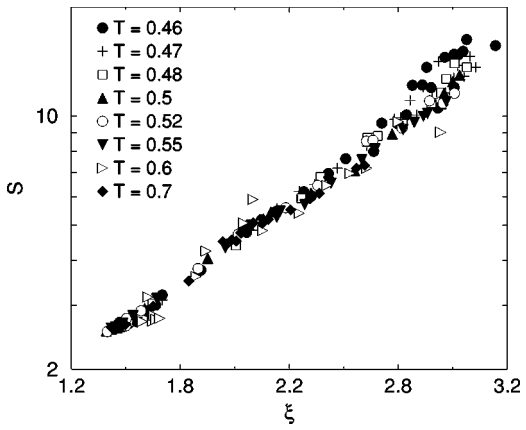

FIG. 14. The weight-averaged mean cluster size S as a function of the characteristic length ξ plotted on a semilogarithmic scale for different T.

system size, which restricts n to only relatively small clusters, and hence skews the estimated exponent in an uncontrolled way. Alternatively, or possibly in addition, the value of τ may simply be different from that expected from percolation theory for *static* clusters, since the clusters we study are intrinsically *dynamic* (i.e., a dynamic criterion is used to define the monomers that make up the clusters, although a static ''snapshot'' is used to analyze the clusters). However, even for static clusters there is experimental evidence for $\tau = 1.4 \pm 0.15$ [73]. As an independent test of τ, percolation theory also predicts a power law relation between the z-average radius of gyration (proportional to ξ) and the weight-average molecular weight (proportional to S) with exponent τ [74–76]. However, for our system, as is shown in Fig. 14, we do not observe a power law relation between ξ and S; rather, we find a roughly exponential relation. Recall that we also find an exponential T dependence for $S(\Delta t_{max})$, rather than a power law. This complicates the attempt to determine τ independently.

A number of other works [16,10,77,78] that study different binary liquids have also calculated a dynamic correlation length, and it is instructive to compare our result with those. Reference [16] calculates the static structure factor for particle pairs whose ''bond'' has been broken, with a dynamic bond criterion based on particle separation. Using the Ornstein-Zernike formalism [79], they extract a static correlation length for particle pairs with broken bonds. This correlation length is not unlike ours, since for particles to have broken a ''bond'' they must have moved apart from each other. The main difference is the absence of a well-defined time scale on which this motion occurs. Reference [16] finds that the correlation length defined in that way grows with decreasing T, but saturates at low T because the correlation length approaches the system size, very similar observations to ours.

References [7,10,77] calculate pair correlation functions based on the deviation of the displacement of each particle from the average value as a function of Δt. Reference [77] finds that the tail of the spatial correlation function can be fitted by an exponential, and from this a correlation length is extracted. Unlike the length calculated in the present work,

and that calculated in Ref. [10], the correlation length of Ref. [77] was found to saturate at a (roughly) constant value at times much longer than the α relaxation time. The behavior observed in Ref. [77] is surprising, since it implies that there exist *persistent* spatial correlations in the particle motion on time scales that exceed all other relaxation times, unexpected for an ergodic liquid. We note that, although in the present work we do find some ''saturation'' of the correlation length around the peak time at low T (possibly due to finite- size effects as discussed above), the length decreases at long times (and must decrease to its ''random'' value at sufficiently long times when the liquid is diffusive).

Lastly, Ref. [78] calculates a dynamical correlation length associated with a four-point space- and time-dependent density correlation function, which emphasizes the least mobile particles in a time window Δt. The correlation length measured shows qualitatively similar behavior to the ξ we measure; in particular, it grows and decreases with Δt, but displays no tendency for saturation at the largest value at long time, possibly due to the larger system size studied there or the absence of polymer-specific effects.

VIII. CONCLUSION

In this paper, we studied the cooperative molecular rearrangement of polymer chains approaching the mode-coupling transition temperature. By focusing on the most highly mobile segments of the chains in a given time window, we observed that these segments, or monomers, form clusters that ''grow'' and ''shrink'' in time. A previous study of this system found that the spatial correlation of scalar monomer displacements is time dependent [8]; this is consistent with the present results. We found that the maximum size of the clusters, as measured by both the number of monomers contained in the cluster and the cluster correlation length, increases with decreasing T. Our results are consistent with those found for a binary LJ liquid [5], and for a colloidal suspension [31].

Our results are also consistent with the premise on which the Adam-Gibbs-DiMarzio theory is based—that the relaxation of a liquid above its glass transition occurs through the cooperative rearrangement of groups of particles (or in the present case chain segments), which grow in size on cooling. We find that the time interval $\Delta t_{\max}$ when the clusters are largest increases on cooling, consistent with the idea that molecular rearrangements become increasingly difficult, requiring the participation of more and more molecules. This time scale is found to follow a scaling law similar to that of the β time scale t_ϵ predicted by MCT, i.e., the exponents obtained from $\Delta t_{\max}$ and t_ϵ by fitting them to a power law are found to be the same within numerical uncertainty. It would be valuable to check if this correspondence between $\Delta t_{\max}$ and t_ϵ is valid across the spectrum of supercooled liquids, or if it is special to the polymer melt we consider.

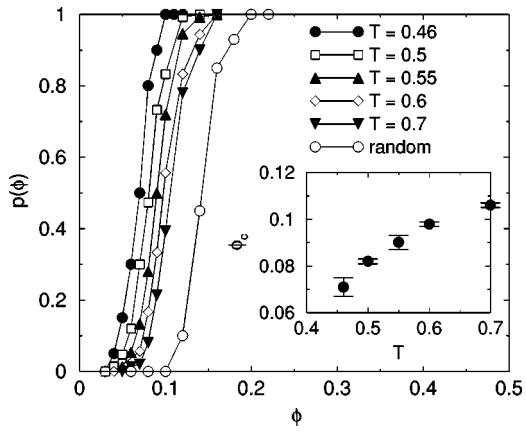

FIG. 15. Percolation probability $p(\phi)$ for different T at $\Delta t = \Delta t_{\max}$. The inset shows the percolation threshold ϕ_c plotted as a function of T. The error bars are obtained from the uncertainties that result due to errors in estimating $\Delta t_{\max}$.

We find that $\Delta t_{\max}$ corresponds to the time scale when the mean square displacement shows a crossover from the ''caging'' regime to the subdiffusive regime. Because this crossover marks the time scale when the monomers are most likely to escape their cages, this correspondence strongly suggests that clustering is required for the cage-breaking process. Since $\Delta t_{\max}$ is much smaller than the α relaxation time τ_α, which marks the time scale for the structural relaxation of the system, our studies suggest that a collection of cooperative molecular rearrangements must give rise to the eventual primary relaxation of the system, consistent with the prediction of MCT.

Our results are also consistent with confocal microscopy experiments on dense colloidal suspensions near their density-driven glass transition, which confirmed the clustering of the most highly mobile particles in the fluid in some time window, as predicted by simulation, and showed the dynamic nature of this clustering. Indeed, such systems are ideal for further exploring cooperative motion in model glass-forming liquids, since it is possible to directly image individual particle trajectories, unlike in experiments on molecular or polymeric liquids [80,81].

ACKNOWLEDGMENTS

We acknowledge useful discussions with N. Lačević, M. Rubinstein, Y. Shim, and J. F. Douglas.

APPENDIX A: PERCOLATION OF MOBILE MONOMERS

In order to demonstrate that the fraction ϕ we use in calculating S is below the percolation threshold ϕ_c, we cal-

TABLE III. Percentage of end monomers that belong to the subset of mobile monomers at the time $\Delta t_{\max}$ when S is maximum.

T	0.46	0.47	0.48	0.5	0.52	0.55	0.6	0.7
%	20.6±0.1	21.3±0.6	21.4±0.1	21.3±0.3	21.4±0.4	22.1±0.2	22±0.2	22.5±0.1

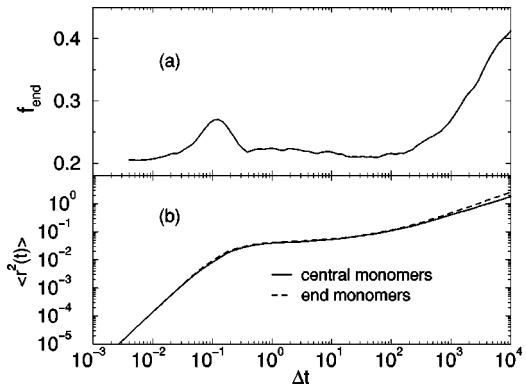

FIG. 16. (a) Fraction of end monomers f_{end} within the subset containing the 6.5% most mobile monomers, as a function of time for $T=0.46$. (b) Mean square displacements of end monomers and non end monomers at $T=0.46$.

culate the probability $p(\phi)$ that a cluster of mobile monomers percolates (spans the system) at a fraction ϕ, and from that estimate ϕ_c. We define a cluster as percolating if it connects any two opposite faces of the box. We define the percolation probability p as the fraction of configurations containing at least one spanning cluster. The percolation threshold ϕ_c can be estimated by the maximum slope of $p(\phi)$, or by $p(\phi_c)\equiv\frac{1}{2}$ [82]. A plot of $p(\phi)$ for each T is shown in Fig. 15. Since the formation of clusters is time dependent, we calculate $p(\phi)$ at the time $\Delta t_{\max}$ when the cluster size is largest and hence the greatest number of spanning clusters exist. For the sake of comparison, we show $p(\phi)$ for a randomly chosen subset of monomers to indicate the value of p one would expect in the absence of dynamical correlations. The random percolation threshold estimated from this calculation is $\phi_{c,rand}=14.4\%$.

For the lowest T, we estimate $\phi_c=(7.1\pm0.4)\%$. The percolation threshold in this system is T dependent, and increases with increasing T (see inset of Fig. 15), giving a larger upper limit for ϕ_c at higher T. At each T, ϕ_c is greater than the ϕ we use to evaluate $S(\Delta t)$.

APPENDIX B: CONTRIBUTION DUE TO MOTION OF END MONOMERS

For sufficiently long time scales, it is known that monomers at the end of a chain are more mobile than those in the middle of the chain [83]. Hence we check whether the mobile monomers are dominated by end monomers on the time scale where the clustering is most pronounced; that is, out of the top 6.5% most highly mobile monomers in $\Delta t_{\max}$, how many of them are end monomers? If the mobility is dominated by the end monomers, we would expect the percentage of end monomers to be much larger than 20%, the percentage one finds by randomly choosing monomers for the ten-mer chains studied here.

For each T, at $\Delta t=\Delta t_{\max}$, the fraction of end monomers within the mobile monomer subset is found to be in the range from 20.6% to 22.5% (Table III), demonstrating systematic but not substantial deviation from the random value. However, as the system reaches the subdiffusive regime as shown by the mean square displacement of monomers, the end monomers should comprise a larger fraction of the mobile monomer subset than their mean field value.

Figure 16(a) shows the percentage of end monomers within the mobile monomer subset as a function of time for $T=0.46$. As can be seen from the figure, during the period when the mean square displacement is in the ballistic or plateau regime, the contribution of end monomers to the fraction of mobile monomers is roughly the same as the mean field value. During these time scales, the monomers ''rattle'' within their local environment, and so the bonds do not have much effect on their mobility, and the end monomers are as constrained as central monomers. But as the monomers break out of their cages and move to larger distances, the contribution of end monomers to the mobile monomers greatly increases. This is also reflected in the mean square displacements calculated using only end monomers and only central monomers [Fig. 16(b)]. For Δt corresponding to a transition between the ballistic regime and the plateau regime, we find a sudden jump in the fraction of end monomers. This indicates the tendency of enhanced mobility of the end monomers just before they become trapped in the cage of their neighbors.

[1] P. G. Debenedetti, *Metastable Liquids: Concepts and Principles* (Princeton University Press, Princeton, NJ, 1996).
[2] M.D. Ediger, C.A. Angell, and S.R. Nagel, J. Phys. Chem. **100**, 13 200 (1996).
[3] W. Kob, C. Donati, S.J. Plimpton, P.H. Poole, and S.C. Glotzer, Phys. Rev. Lett. **79**, 2827 (1997).
[4] C. Donati, J.F. Douglas, W. Kob, S.J. Plimpton, P.H.Poole, and S.C. Glotzer, Phys. Rev. Lett. **80**, 2338 (1998).
[5] C. Donati, S.C. Glotzer, P.H. Poole, W. Kob, and S.J. Plimpton, Phys. Rev. E **60**, 3107 (1999).
[6] S.C. Glotzer and C. Donati, J. Phys.: Condens. Matter **11**, A285 (1999).
[7] C. Donati, S.C. Glotzer, and P.H. Poole, Phys. Rev. Lett. **82**, 5064 (1999).
[8] C. Bennemann, C. Donati, J. Baschnagel, and S.C. Glotzer, Nature (London) **399**, 246 (1999).
[9] P.H. Poole, C. Donati, and S.C. Glotzer, Physica A **261**, 51 (1998).
[10] S. C. Glotzer, C. Donati, and P. H. Poole, in *Computer Simulation Studies in Condensed Matter Physics XI*, edited by D. P. Landau, (Springer-Verlag, Berlin, 1999).
[11] P. Allegrini, J.F. Douglas, and S.C. Glotzer, Phys. Rev. E **60**, 5714 (1999).
[12] A. Heuer and K. Okun, J. Phys. Chem. **106**, 6176 (1997).
[13] B. Doliwa and A. Heuer, Phys. Rev. Lett. **80**, 4915 (1998).
[14] Y. Hiwatari and T. Muranaka, J. Non-Cryst. Solids **235**, 19 (1998).
[15] D.N. Perera and P. Harrowell, J. Non-Cryst. Solids **235**, 314 (1998).
[16] R. Yamamoto and A. Onuki, Phys. Rev. E **58**, 3515 (1998).

[17] D.N. Perera and P. Harrowell, J. Chem. Phys. **111**, 5441 (1999).
[18] G. Johnson, A.I. Mel'cuk, H. Gould, W. Klein, and R.D. Mountain, Phys. Rev. E **57**, 5707 (1998).
[19] K. Schmidt-Rohr and H.W. Spiess, Phys. Rev. Lett. **66**, 3020 (1991).
[20] A. Heuer, M. Wilhelm, H. Zimmerman, and H. W. Spiess, Phys. Rev. Lett. **75**, 2851 (1995).
[21] I. Chang, F. Fujara, B. Geil, G. Heuberger, T. Mangel, and H. Sillescu, J. Non-Cryst. Solids **172-174**, 248 (1994).
[22] G. Heuberger and H. Sillescu, J. Phys. Chem. **100**, 15 255 (1996).
[23] U. Tracht, M. Wilhelm, A. Heuer, H. Feng, K. Schmidt-Rohr, and H.W. Spiess, Phys. Rev. Lett. **81**, 2727 (1998).
[24] A.H. Marcus, J. Schofield, and S.A. Rice, Phys. Rev. E **60**, 5725 (1999).
[25] M.T. Cicerone and M.D. Ediger, J. Chem. Phys. **103**, 5684 (1995).
[26] B. Schiener, R.V. Chamberlin, G. Diezemann, and R. Bohmer, J. Chem. Phys. **107**, 7746 (1997).
[27] G. Hinze, Phys. Rev. E **57**, 2010 (1998).
[28] J. Leisen, K. Schmidt-Rohr, and H.W. Spiess, Physica A **201**, 3020 (1993); R. Böhmer, G. Hinze, G. Diezemann, B. Geil, and H. Sillescu, Europhys. Lett. **36**, 55 (1996); S.C. Kuebler, A. Heuer, and H.W. Spiess, Phys. Rev. E **56**, 741 (1997); R. Böhmer, G. Diezemann, G. Hinze, and H. Sillescu, J. Chem. Phys. **108**, 890 (1998).
[29] M.D. Ediger, Annu. Rev. Phys. Chem. **51**, 99 (2000).
[30] W.K. Kegel and A.V. Blaaderen, Science **287**, 290 (2000).
[31] E. Weeks, J.C. Crocker, A.C. Levitt, A. Schofield, and D.A. Weitz, Science **287**, 627 (2000).
[32] R. Böhmer *et al.*, J. Non-Cryst. Solids **235**, 1 (1998).
[33] F.H. Stillinger and J.A. Hodgdon, Phys. Rev. E **50**, 2064 (1994).
[34] R. Böhmer, Curr. Opin. Solid State Mater. Sci. **3**, 378 (1998).
[35] H. Sillescu, J. Non-Cryst. Solids **243**, 81 (1999).
[36] S.C. Glotzer, J. Non-Cryst. Solids **274**, 342 (2000).
[37] M.T. Cicerone, F.R. Blackburn, and M.D. Ediger, Macromolecules **28**, 8224 (1995).
[38] D.D. Deppe, A. Dhinojwala, and J.M. Torkelson, Macromolecules **29**, 3898 (1996).
[39] E. Hemple, G. Hemple, A. Hensel, C. Schick, and E. Donth, J. Phys. Chem. B **104**, 2460 (2000).
[40] E. Leutheusser, Phys. Rev. A **29**, 2765 (1984); U. Bengtzelius, W. Götze, and A. Sjölander, J. Phys. C **17**, 5915 (1984); W. Götze and L. Sjögren, Rep. Prog. Phys. **55**, 241 (1992); Chem. Phys. **212**, 47 (1996); Transp. Theory Stat. Phys. **24**, 801 (1995).
[41] T.B. Schrøder, S. Sastry, J.C. Dyre, and S.C. Glotzer, J. Chem. Phys. **112**, 9834 (2000).
[42] E. La Nave, A. Scala, F.W. Starr, F. Sciortino, and H.E. Stanley, Phys. Rev. Lett. **84**, 4605 (2000); L. Angelani, R. Di Leonardo, G. Ruocco, A. Scala, and F. Sciortino, *ibid.* **85**, 5356 (2000); K. Broderix, K.K. Bhattacharya, A. Cavagna, A. Zippelius, and I. Giardina, *ibid.* **85**, 5360 (2000).
[43] C.A. Angell, Science **267**, 1924 (1995); C.A. Angell, K.L. Ngai, G.B. McKenna, P.F. McMillan, and S.W. Martin, J. Appl. Phys. **88**, 3113 (2000).
[44] M. Goldstein, J. Chem. Phys. **51**, 3728 (1969).
[45] C. Bennemann, W. Paul, K. Binder, and B. Dünweg, Phys. Rev. E **57**, 843 (1998); C. Bennemann, W. Paul, J. Baschnagel, and K. Binder, J. Phys.: Condens. Matter **11**, 2179 (1999); J. Baschnagel, C. Bennemann, W. Paul, and K. Binder, *ibid.* **12**, 6365 (2000); C. Bennemann, J. Baschnagel, and W. Paul, Eur. Phys. J. B **10**, 323 (1999); M. Aichele and J. Baschnagel, Eur. Phys. J. E **5**, 229 (2001); **5**, 245 (2001).
[46] T.B. Schrøder and J.C. Dyre, J. Non-Cryst. Solids **235**, 331 (1998); F.W. Starr, F. Sciortino, and H.E. Stanley, Phys. Rev. E **60**, 6757 (1999); H. Miyagawa, Y. Hiwatari, B. Bernu, and J.P. Hansen, J. Chem. Phys. **88**, 3879 (1988); G. Wahnström, Phys. Rev. A **44,** 3752 (1991).
[47] The mean square displacement shown in Fig. 1 does not reach the diffusive regime on the time scale of the simulations. This is typical behavior for short polymer chains where, beyond the cage regime, $\langle r^2 \rangle$ is subdiffusive until monomers have moved a distance roughly equal to the end-to-end distance R_e of the chains. At distances (and times) greater than $\langle r^2 \rangle \approx R_e^2$, $\langle r^2 \rangle$ shows the diffusive behavior ($\langle r^2 \rangle \approx 6Dt$) found in simple liquids.
[48] K. Kremer and G.S. Grest, J. Chem. Phys. **92**, 5057 (1990).
[49] A. Kopf, B. Dünweg, and W. Paul, J. Chem. Phys. **107**, 6945 (1997).
[50] Note that, according to this procedure, any other choice for Δt^* would result in smaller fractions than the time interval when α_2 is maximum. This is because, at time intervals earlier or later than the time when α_2 is maximum, the deviation of the van Hove correlation function from the Gaussian distribution becomes smaller, resulting in a smaller number of particles in the tail of the distribution. Therefore, ϕ is maximum at Δt^* when α_2 is maximum.
[51] J. P. Hansen and I. R. McDonald, *Theory of Simple Liquids* (Academic, London, 1986).
[52] Although one uses configurations both at $\Delta t = 0$ and at Δt to define monomer mobility, our results are the same regardless of which configuration is used for constructing clusters.
[53] D. A. McQuarrie, *Statistical Mechanics* (Harper and Row, New York, 1976).
[54] D. Stauffer, *Introduction to Percolation Theory* (Taylor and Francis, London, 1985); D. Stauffer and N. Jan (private communication).
[55] The normalization of S_w by S_0 factors out the contribution from random clustering, and allows us to quantify the degree of correlation irrespective of the choice of fraction ϕ.
[56] At much longer times, beyond the scope of these simulations, the diffusive regime is reached.
[57] F. Sciortino, P. Gallo, P. Tartagila, and S.H. Chen, Phys. Rev. E **54**, 6331 (1996).
[58] K. Binder *et al.*, in *Complex Behavior of Glassy Systems*, edited by M. Rubi and C. Perez-Vicente (Springer, Berlin, 1997); W. Kob, J. Phys.: Condens. Matter **11**, A1 (1999).
[59] W. Götze, J. Phys.: Condens. Matter **11**, A1 (1999).
[60] F. Sciortino and P. Tartaglia, J. Phys.: Condens. Matter **11**, A261 (1999).
[61] G. Adam and J.H. Gibbs, J. Chem. Phys. **43**, 139 (1965).
[62] J.H. Gibbs and E.A. DiMarzio, J. Chem. Phys. **28**, 373 (1958).
[63] J.H. Gibbs, J. Chem. Phys. **25**, 185 (1956).
[64] E.A. DiMarzio and J.H. Gibbs, J. Chem. Phys. **28**, 807 (1958).
[65] E.J. Donth, J. Non-Cryst. Solids **53**, 325 (1982); **131-133**, 204

(1991); *Relaxation and Thermodynamics in Polymers: Glass Transition* (Akademie-Verlag, Berlin, 1992); C.T. Moynihan and J. Schroeder, J. Non-Cryst. Solids **160**, 52 (1993); **161**, 148 (1993); U. Mohanty, Adv. Chem. Phys. **89**, 89 (1995); J. Chem. Phys. **100**, 5905 (1994); R.E. Robertson, J. Polym. Sci., Polym. Symp. **63**, 173 (1978); M.D. Ediger, J. Non-Cryst. Solids **235-237**, 10 (1998).

[66] D. Sappelt and J. Jäckle, J. Phys. A **26**, 7325 (1993); C. Donati and J. Jäckle, J. Phys.: Condens. Matter **8**, 2733 (1996).

[67] R.J. Speedy, J. Phys. Chem. B **103**, 4060 (1999).

[68] M. Mézard and G. Parisi, J. Phys.: Condens. Matter **11**, A157 (1999).

[69] A. Scala, F.W. Starr, E. La Nave, F. Sciortino, and H.E. Stanley, Nature (London) **406**, 166 (2000); F.W. Starr *et al.*, Phys. Rev. E **63**, 041201 (2001).

[70] S. Sastry, Phys. Rev. Lett. **85**, 590 (2000); Nature (London) **409**, 164 (2001).

[71] A. Heuer, Phys. Rev. Lett. **78**, 4051 (1997); S. Buechner and A. Heuer, Phys. Rev. E **60**, 6507 (1999).

[72] Reference [5] found, for a binary LJ mixture, that $S_{\max}$ is reasonably well described (over the limited T range of their simulations) by the form $S_{\max} \sim (T - T_{\mathrm{MCT}})^{-\gamma}$. In contrast, the present data do not show a good power law fit for $T_{\mathrm{MCT}} = 0.45$; instead, we find that $S_{\max}$ can be fitted with a power law of the form $(T - T_p)^{-\gamma}$ with $T_p = 0.28$, a temperature substantially lower than T_{MCT}. We point out that Ref. [5] studied a much larger system, where finite size effects are presumably less pronounced. The relatively small size of our system might contribute to the difference we find between T_p and T_{MCT}, but further simulations are required to test this.

[73] G.K. von Schulthess, G.B. Benedek, and R.W. De Blois, Macromolecules **13**, 939 (1980).

[74] M. Daoud, F. Family, and J. Jannink, J. Phys. (France) Lett. **45**, L199 (1984).

[75] E.V. Patton, J.A. Wesson, M. Rubinstein, J.C. Wilson, and L.E. Oppenheimer, Macromolecules **22**, 1946 (1989).

[76] M. Rubinstein (private communication).

[77] B. Doliwa and A. Heuer, Phys. Rev. E **61**, 6898 (2000).

[78] N. Lačević, R. W. Starr, T. B. Schroder, V. N. Novikov, and S. C. Glotzer (unpublished).

[79] H. E. Stanley, *Introduction to Phase Transitions and Critical Phenomena* (Oxford University Press, New York, 1971).

[80] S.C. Glotzer, Phys. World **13**, 22 (2000).

[81] M. Ediger, Science **287**, 604 (2000).

[82] S.A. Safran, I. Webman, and Gary S. Grest, Phys. Rev. A **32**, 506 (1985).

[83] M. Doi and S. F. Edwards, *Theory of Polymer Dynamics* (Wiley, New York, 1987).